Structural Basis of Disease-Causing Mutations in Hepatocyte Nuclear Factor 1β[†,‡]

Peng Lu, Geun Bae Rha, and Young-In Chi*

Department of Molecular and Cellular Biochemistry, Center for Structural Biology, University of Kentucky, Lexington, Kentucky 40536

Received May 29, 2007; Revised Manuscript Received August 8, 2007

ABSTRACT: HNF1β is an atypical POU transcription factor that participates in a hierarchical network of transcription factors controlling the development and proper function of vital organs such as liver, pancreas, and kidney. Many inheritable mutations on *HNF1β* are the monogenic causes of diabetes and several kidney diseases. To elucidate the molecular mechanism of its function and the structural basis of mutations, we have determined the crystal structure of human HNF1β DNA binding domain in complex with a high-affinity promoter. Disease-causing mutations have been mapped to our structure, and their predicted effects have been tested by a set of biochemical/ functional studies. These findings together with earlier findings with a homologous protein HNF1α, help us to understand the structural basis of promoter recognition by these atypical POU transcription factors and the site-specific functional disruption by disease-causing mutations.

HNF1β (hepatocyte nuclear factor 1β; also known as vHNF1 or TCF2) is a widely distributed transcription factor that plays a critical role in early vertebrate development and embryonic survival (*1*−*3*). First identified as a key regulator in the liver, HNF1β is also expressed in the pancreas, kidney, lung, ovary, testis, and throughout the gastrointestinal tract. In pancreatic β-cells, HNF1β is known to form an integrated regulatory network with other transcription factors such as HNF1α, HNF4α, Pdx-1, Foxa2, and NeuroD1 for organ development and proper function (*1*, *4*). Thus, in humans, heterozygous mutations in the HNF1β gene have been linked to neonatal diabetes (*5*) and the autosomal dominant subtype of diabetes known as MODY (maturity-onset diabetes of the young) (*6*). Extrapancreatic diseases are also increasingly recognized in different organs, especially in the kidney, with a variety of renal developmental disorders such as renal cysts, familial hypoplastic glomerulocystic kidney disease, renal malformation, and atypical familial hyperuricaemic nephropathy (*7*−*11*).

POU transcription factors, which include *P*it-1, *O*ct-1, and *U*nc-86 as founding members and are now expanded to more than 13 members in humans, are developmental regulators of various neuroendocrine organs, and their sequence-specific DNA binding is mediated by a bipartite motif that consists of a POU homeodomain (POU_H) and POU-specific domain (POU_S) (*12*, *13*). POU_H is a 60 amino acid classic homeodomain made of three α-helices with the third as a DNA recognition helix, while POU_S is an additional ∼75 amino acid all-α-helical motif that cooperates with POU_H to enhance the binding affinity and specificity of DNA binding (Figures 1 and 2) (*12*, *14*). HNF1α (MODY3 gene product, the most commonly mutated MODY protein) and HNF1β (MODY5 gene product) are atypical members of the POU transcription factors. Their POU_S domains have at least one additional α-helix at the N-terminus, and the second helix and adjacent loop of their POU_H domains are much longer, creating a more extensive interface between the POU_S and POU_H domains (Figure 2) (*15*). This extended interface fixes the relative orientations of the two domains and provides rigidity for DNA recognition (*15*) as opposed to the flexibility seen in another POU transcription factor, Pit-1. The interdomain interaction in Pit-1 is relatively minimal, which allows it to adopt unique conformations when binding to different promoters and provides an allosteric mechanism by recruiting distinct subsets of coactivators and corepressors (*16*). Another distinction comes from the fact that while other POU transcription factors such as Oct-1 and Pit-1 can bind DNA as either monomers or dimers (*12*, *14*), HNF1α and HNF1β bind DNA exclusively as dimers.

HNF1α and HNF1β are encoded by two different genes (*HNF1α* on 12q22-qter and *HNF1β* on 17cen-q21.3), and they are functionally distinct. For example, the timing and tissue-specificity of their gene expression appear to be quite different: that is, HNF1β is expressed in pancreatic stem cells before differentiation into endocrine or exocrine cells (*17*), while HNF1α is primarily involved in maintaining proper function of vital organs (*18*−*20*). In addition, distinctive sets of MODY mutations are found in *HNF1α* and *HNF1β* (*21*, *22*), and the phenotypes between the patients with *HNF1α* and *HNF1β* mutations are markedly different (*23*). Even though mutations in both are associated with diabetes, renal developmental disorders and genital malformations are more prominent with the mutations in *HNF1β* (*7*, *8*), which also encompass a wide clinical spectrum including genital tract malformations, abnormal liver function, pancreatic atrophy, exocrine insufficiency, and

[†] This work was funded by the Juvenile Diabetes Research Foundation (1-2004-506) to Y.-I.C. and by NIH Grant P20RR20171 from the COBRE program of the National Center for Research Resources (NCRR).

[‡] Coordinates and structure factors have been deposited in the RSCB Protein Data Bank under accession code 2H8R.

* To whom correspondence should be addressed: phone 859-323-5493; fax 859-257-2283; e-mail ychi@uky.edu.

10.1021/bi7010527 CCC: $37.00
Published on Web 10/09/2007

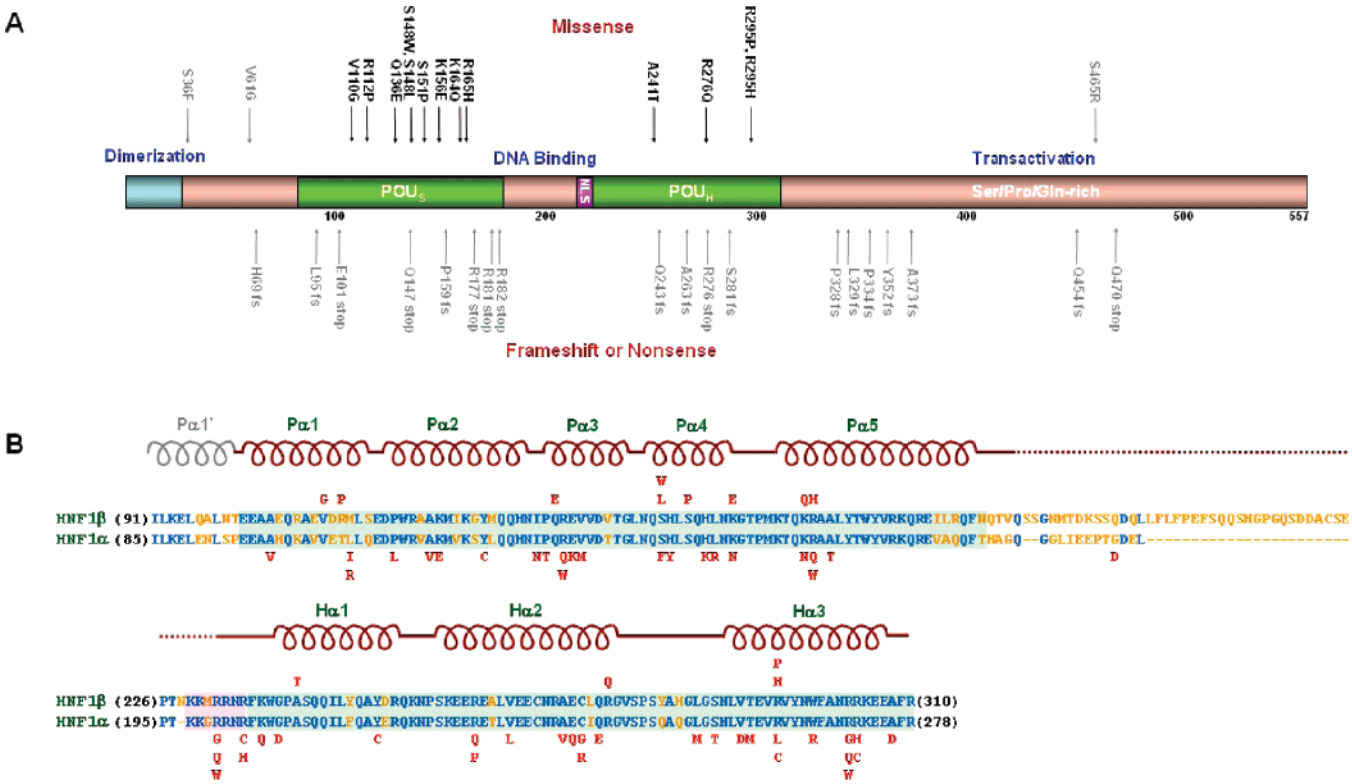

FIGURE 1: (A) Disease-causing mutations found in HNF1β. Unlike nonsense and frameshift mutations, point mutations are clustered within the DNA binding domain. Point mutations found in the DNA binding domain are indicated in black, and the remaining regions are shown in gray. (B) Sequence alignment of human HNF1β and HNF1α DNA binding domains. Pα1 through Pα5 make up POU$_S$, while Hα1 through Hα3 make up POU$_H$. Invariant and variant residues are colored blue and brown, respectively. Point mutations are shown in red above (HNF1β) and below (HNF1α) the sequences. The numbers in front of each sequence indicate the beginning number of the amino acids, and the core domains and the nuclear localization signal (NLS) are highlighted by green and pink shadow boxes, respectively.

biliary manifestations (*8*, *24*). Recently, HNF1β has also been associated with ovarian clear cell carcinoma (*25*, *26*), and mutations in this protein are also responsible for neonatal cholestatic jaundice (*27*). Thus, in addition to its effect on pancreatic β-cells (*5*, *28*, *29*), HNF1β appears to be involved in normal functioning of many other organs (*10*, *11*).

Human HNF1β is made of 557 amino acids and, like HNF1α, it has three distinctive modular domains: the dimerization domain, which is further stabilized by a dimerization cofactor DcoH; the POU DNA binding domain; and the transactivation domain (Figure 1). Amino acid sequences are highly conserved only in the dimerization and DNA binding domains. Variable linkers between the domains and the diverse C-terminal transactivation domain are believed to facilitate interactions with different sets of proteins for HNF1α and HNF1β. Despite sequence similarity in the DNA binding domains, HNF1β and HNF1α have apparently different target gene selectivity within the same cells. For example, in kidney cells, 25 potential target genes have been identified for HNF1β while only nine (three common and six unique ones) have been identified for HNF1α (*30*). While the structural and functional properties of HNF1α have been extensively studied, the structural features of HNF1β remain essentially uncharacterized and are mainly inferred from its homology to HNF1α. Thus, to gain additional insight into the molecular basis of target gene recognition by these POU transcription factors and the functional disruption made by disease-causing mutations, we have determined the crystal structure of human HNF1β DNA binding domain in complex with a high-affinity promoter and functionally characterized the mutations that are found in this mutational 'hot-spot' region.

MATERIALS AND METHODS

Structure Determination and Refinement. Preparation of the samples and crystallization of the complex have been reported previously (*31*). The crystals belong to the space group *R*3 with unit cell dimensions $a = b = 174.69$ Å and $c = 72.43$ Å and diffraction to 3.2 Å resolution. There is one complex (two HNF1β and one dsDNA) in the crystal asymmetric unit (62% solvent content). The structure was solved by the molecular replacement method by use of MOLREP (*32*). As a search model, we used our previous structure of HNF1α/DNA complex (*15*). The best solution had a correlation coefficient of 52.4%, 15.2% above the second-best solution. The R_{cryst} value after molecular replacement was 0.51. After one round of rigid-body refinement, R_{cryst} and R_{free} dropped to 0.43 and 0.44, respectively. Protein residues were changed in order to match the sequence of HNF1β and the model was refined by simulated annealing implemented in CNS (*33*). Model building was done with O (*34*), and refinement was continued by simulated annealing with CNS, with restraints placed on bond lengths, bond angles, nonbonded contacts, and temperature factors of neighboring atoms. Noncrystallographic symmetry (NCS) restraints were imposed only on the protein, and bulk-solvent corrections were applied. The σA-weighted $2F_o - F_c$ maps as well as omit maps were calculated at regular intervals to allow manual rebuilding. Inclusion of individual atomic

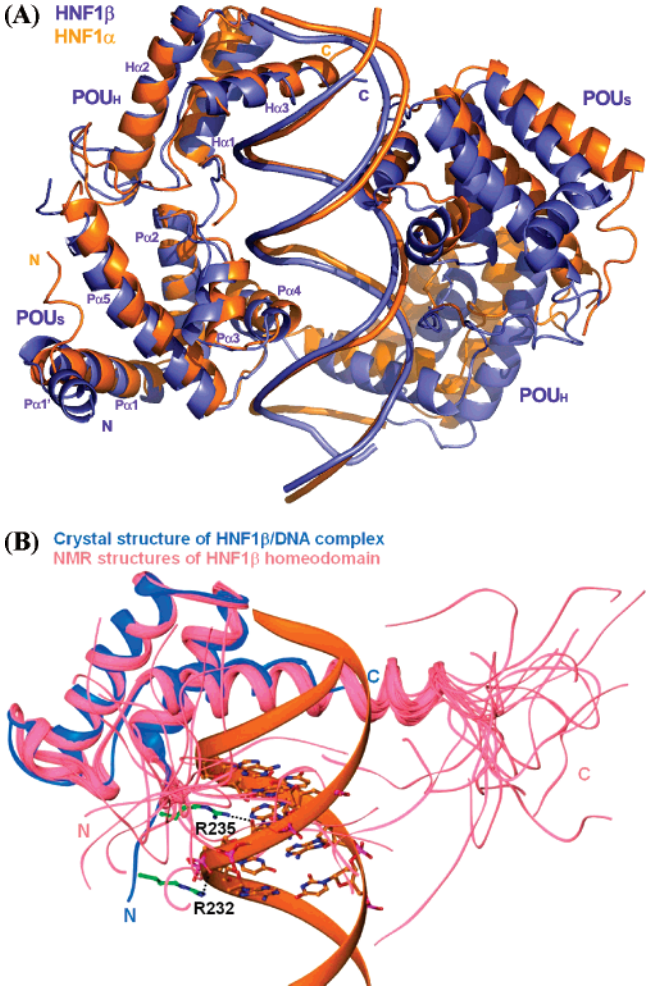

FIGURE 2: (A) Comparison of HNF1β-DNA (purple) and HNF1α-DNA (gold) (*60*) complexes. The two structures are superimposed through their POU_H domains of the first molecule (left). After the operation, the POU_S domains of the first molecule also superimpose very well, while the second molecules are 9.8° apart from each other. (B) Superposition of HNF1β homeodomain/DNA complex crystal structure (blue) with the NMR ensemble structures of HNF1β homeodomain without DNA (pink, PDB code 2DA6). The N-terminal arm containing two key arginine residues (R235 and R232) that make contacts with DNA through the minor groove can be seen below the helices on the left.

temperature factors and removal of NCS restraints during the final stages of refinement were accompanied by a substantial decrease in R_{free} values. The final refinement statistics are provided in Table 1.

Site-Directed Mutagenesis. The Quick Change Multi Site-Directed Mutagenesis kit (Stratagene) was used to generate constructs with point mutations of HNF1β DNA binding domain according to the manufacturer's instructions. The plasmid templates used in the mutagenesis protocol were pET41a GST-HNF1β DBD and pCMV-SPORT6 HNF1β (Mammalian Gene Collection 21262). All of the generated constructs with the mutated sequences were verified with DNA sequencing.

Electromobility Shift Assay. Standard gel mobility-shift assays (EMSA) (*35*) were used to determine the effects of disease-causing mutations on binding affinity for DNA recognition sites. Briefly, binding reactions of different protein:DNA molar ratios were assembled at 25 °C in a total volume of 10 μL in 10 mM Tris, pH 7.5, 50 mM NaCl, 1

Table 1: Data and Refinement Statistics

Native Diffraction Data		
parameter	total	outer shell
resolution (Å)	27.9−3.2	3.31−3.20
R_{merge}[a] (%)	8.3	29.2
completeness (%)	94.3	63.4
$I/\sigma(I)$	28.8	3.4
redundancy	6.3	3.8
Refinement		
no. of reflections (20.0−3.2 Å)		
work	11,992	
free-flag[b]	637	
modeled regions	aa 90−187 and 231−308 in molecule A aa 90−185 and 231−310 in molecule B DNA 1−20 in chain E and 2−21 in chain F	
R factor (%)	22.9	
R_{free} (%)	28.7	
$\langle B \rangle$ for all atoms (Å^2)	69.45	
rms deviations		
bond lengths (Å)	0.079	
bond angles (deg)	5.45	

[a] $R_{merge} = \Sigma_h \Sigma_i |I(h)_i - \langle I(h) \rangle| / \Sigma_h \Sigma_i I(h)_i$, where $I(h)$ is the intensity of reflection h, Σ_h is the sum over all reflections, and Σ_i is the sum over i measurements of reflection h. [b] 5% of the reflection data excluded from refinement.

mM $MgCl_2$, 0.5 mM dithiothreitol (DTT), 0.5 mM ethylenediaminetetraacetic acid (EDTA), 100 μg/mL bovine serum albumin (BSA), 10 μg/mL poly(dI-dC), and 4% (v/v) glycerol. Purified protein was incubated in the binding buffer at 25 °C for 10 min before the addition of oligo-DNA. Reaction mixtures were incubated at 25 °C for an additional 20 min before they were loaded onto a 6% nondenaturing polyacrylamide gel that had been pre-run at 4 °C for 30 min in 0.5× TBE (45 mM Tris, 45 mM borate, and 1 mM EDTA, pH 8.3). Electrophoresis continued for about an hour before the gel was stained with 0.1 μg/mL ethidium bromide in 0.5× TBE buffer. For these experiments, we used the same oligo (21-mer overhang) that was used for crystallization and structure determination (*31*).

Cell Culture. HeLa cell line was cultured in Dulbecco's modified Eagle medium (DMEM) supplemented with 10% fetal bovine serum (Invitrogen), 50 units/mL penicillin G, 50 μg/mL streptomycin (Sigma), and 0.1 mM nonessential amino acids (Invitrogen).

Transcription Assays (Luciferase Reporter Assays). Three copies of the HNF1β binding element from the β-fibrinogen promoter [pGL3-(β28)$_3$] were subcloned into the firefly luciferase reporter vector pGL3-Basis (Promega). The Quick Change Multi Site-Directed Mutagenesis kit (Stratagene) was used to create specific substitutions, and all sequences were verified. HeLa cells were transfected by use of Opti-MEM and LipofectAMINE 2000 reagent (Invitrogen) according to the manufacturer's recommendations. Briefly, a total of 50 ng of pCMV-SPORT6 HNF1β or mutants, 50 ng of pGL3-(β28)$_3$ and 5 ng of pRL-TK (control *Renilla* luciferase vector) were used for transfection of 1×10^5 cells seeded on a 24-well plate 1 day before transfection. Forty-eight hours after transfection, cells were washed with 1× PBS and lysed with luciferase lysis buffer supplied with the luciferase assay kit (Promega). Luciferase activity was measured with the dual luciferase assay system (Promega) and Lmax luminometer (Molecular Devices). All values were normalized by the relative ratio of firefly luciferase activity and *Renilla*

luciferase activity. At least three independent transfections were performed in quadruplicate.

Western Blotting. Immunodetection of expression of HNF1β and mutants in HeLa cells was performed with whole-cell lysates, rabbit anti-HNF1β antibody (Santa Cruz), rabbit anti-actin antibody (Sigma), and goat anti-rabbit antibody conjugated with horseradish peroxidase (HRP) (Cell Signaling Technology). Briefly, transfected cells were lysed with cell lysis buffer (20 mM Tris, pH 7.5, 150 mM NaCl, 0.5% Triton X-100, 0.5% NP-40, and 1 mM EDTA) with protease inhibitors. Cell lysates were centrifuged and protein concentration of each cell lysate was determined by use of Bio-Rad protein assay reagent. The same amounts of cell lysates were loaded onto an SDS−15% polyacrylamide gel and proteins were fractionated by electrophoresis and transferred to poly(vinylidene difluoride) (PVDF) membrane. The blotted membrane was incubated with aforementioned antibodies and signals were detected by an enhanced chemiluminescenc- (ECL-) based method (Amersham).

Protein Stability Assays (Pulse−Chase Experiment). Stability of the mutants in cultured cells was measured by means of pulse−chase experiments. Twenty-four hours after transfection, HeLa cells were serum-starved for 1 h before being incubated in DMEM minus Met/Cys for 30 min and then labeled with 100 μCi/mL Trans ^{35}S labeling mix (MP Biomedicals) for 30 min at 37 °C. Labeling medium was removed thereafter and the ^{35}S-labeled cells were incubated in DMEM medium containing 10% FBS for the indicated periods of time (0−18 h) and lysed. The nuclear extracts were prepared by use of a NucBuster protein extraction kit (Novagen). Proteins were immunoprecipitated with anti-HNF1β antibody (Santa Cruz) and protein A−Sepharose beads (Amersham) and resolved by SDS−PAGE, and incorporated radioactivity was analyzed by autoradiography with BioMax film (Eastman Kodak).

RESULTS AND DISCUSSION

Overall Structure of HNF1β and Comparison with HNF1α. HNF1β and HNF1α share 70% sequence identity within the construct (HNF1β amino acids 91−310) and 82% when the more variable linker between the POU_H and POU_S domains is not considered. As expected, the overall structure of HNF1β is very similar to that of HNF1α with the exception of the very N-terminal end of the constructs, where HNF1β adopts an additional two-turn helix (Pα1′) remote from the DNA binding surface (Figure 2A). HNF1α and HNF1β DNA binding domains superimpose extremely well (Figure 2A); rmsd values for superposition of backbone atoms of the HNF1β POU_H and POU_S (excluding Pα1′) with those of HNF1α are 1.19 and 1.12 Å, respectively. The relative orientation between the two domains is almost identical, owing to the extensive interdomain binding surface that provides rigidity between the two domains. However, when one molecule of each complex is superimposed, the second molecules are rotated by 9.8° with respect to each other (Figure 2A). This offset could be due to different crystal packing or slightly different mode of DNA backbone recognition (Figure 3) or a combination of both. The overall DNA conformations are similar in both complexes.

The extensive interdomain binding surface in HNF1α and HNF1β is quite unusual among POU transcription factors

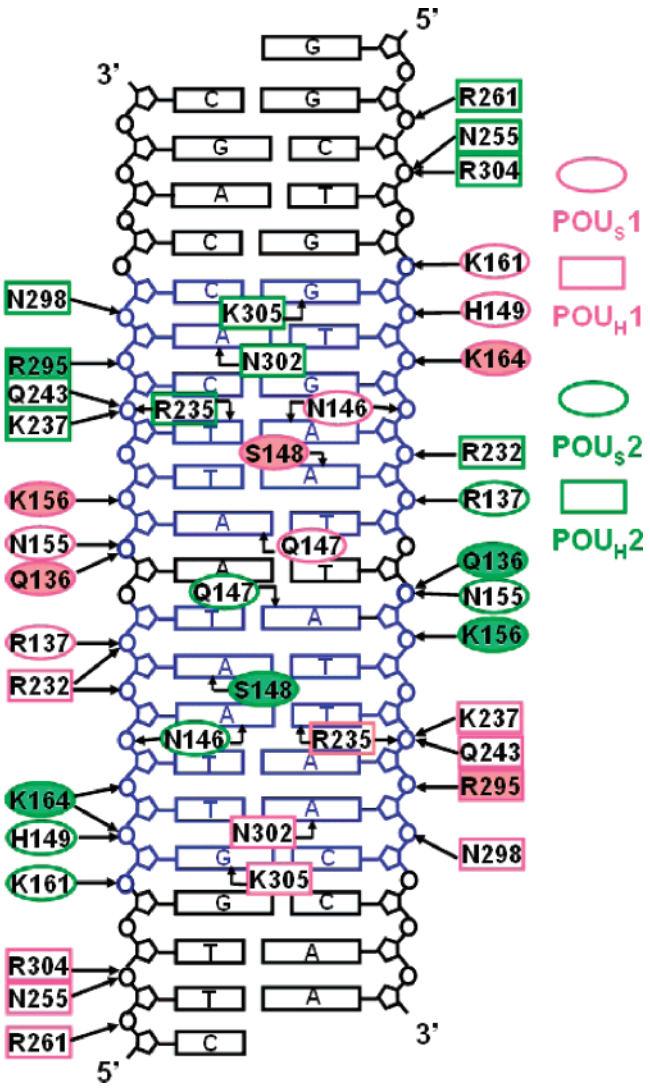

FIGURE 3: Schematic summary of HNF1β−DNA interactions and disease-causing mutations. Residues from molecules 1 and 2 are shown in pink and green, respectively. POU_H and POU_S domain residues are shown as rectangles and ovals, respectively; filled shapes indicate disease-causing mutations. DNA bases within the consensus recognition motif are colored blue.

and plays a key role in optimal target gene recognition (*15*). The contact between the POU_S and POU_H domains in the HNF1β monomer buries even more than what has been observed with the HNF1α structure (474 Å^2 vs 297 Å^2) (Figures 2 and 4). Specific interactions are made by the elements not present in classical POU_H and POU_S domains: the C-terminal extension of Hα2, the longer loop between Hα2 and Hα3, and the C-terminal extension of Pα5. These interactions include the side-chain−side-chain (N133···Q275, R137···N234, Q138···N234, and T186···K282) and side-chain−backbone (Q131···Q275, H132···R276, N133···K237, T186···K282, and Q182···G285) hydrogen bonds and the F183−V278 van der Waals interactions. Unlike HNF1α, no hydrophobic patch is found at the interdomain interface of HNF1β. The intramolecular interface between POU_S and POU_H domains of Pit-1, in contrast, is much smaller, with 92 and 67 Å^2 buried for complexes with prolactin and growth hormone promoters, respectively (*16*). In the case of Pit-1, flexibility between POU_S and POU_H domains allows differential recognition of promoters, which, in turn, is thought to facilitate its association with distinct subsets of coactivators

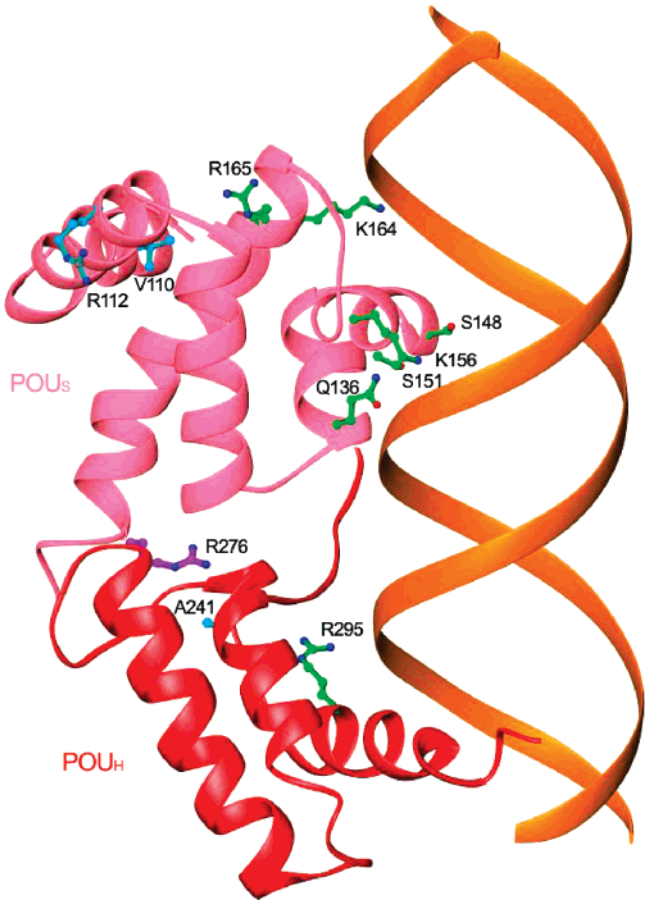

FIGURE 4: Mapping of disease-causing mutations on the HNF1β structure (upside-down view from Figure 2). Ribbon representation of HNF1β is shown in pink (POU_S) or red (POU_H), and DNA is in orange. Side chains of residues affected by diabetes-associated missense mutations are displayed in green (predominantly affecting DNA binding), purple (interdomain interactions), or light blue (protein stability).

and corepressors. The more extended interface between POU_S and POU_H domains indicates the opposite for HNF1α and HNF1β: that rigidity, as opposed to flexibility, might be necessary for normal function. HNF1α and HNF1β recognize a target sequence with only one base pair between the two recognition subsites (Figure 3) while Pit-1 and Oct-1 can recognize the target sequences with different numbers of base pairs in between subsites and accordingly recruit different subsets of coactivators and corepressors (*16*, *36*).

Another unique feature of POU transcription factors is the extended coil region covalently linking POU_S and POU_H domains, whose sequence variability is the key element in differential combinatorial control of gene expression (*37*) by recruiting different sets of transcriptional coregulators (*38*). The linker between the POU_S and POU_H domains (amino acids 186−229) of HNF1β contains the nuclear localization signal (NLS; ^{229}KKMRRNRFK^{237}) and is even longer than that of HNF1α (by 26 residues) (Figure 1). The majority of the linker is disordered, as also seen in the HNF1α structure (*15*). Intrinsically disordered regions are highly abundant in protein structures and frequently mediate protein−protein interactions (*39*, *40*). Transcription factors are no exception (*41*), and the flexible linkers and unstructured C-terminal transactivation domains are believed to mediate multiple protein−protein interactions including the recruitment of transcription coregulators. In HNF1α, this flexible linker is necessary for interaction with CBP/p300 (*42*, *43*).

DNA Recognition by HNF1β. We used the same synthetic double-stranded DNA that corresponds to the consensus motif for optimal binding by both HNF1α and HNF1β (*31*, *44*, *45*) and was used for HNF1α/DNA complex structure determination (*15*). POU_H and POU_S domains of each protomer bind the same face of DNA. The second protein molecule binds in the same fashion to the opposite DNA face and in the reverse orientation. The schematic drawing of HNF1β−DNA interactions is shown in Figure 3.

The hallmarks of DNA−homeodomain and DNA−POU_S interactions are present in our structure (Figures 2 and 3). Helix Hα3 of the homeodomain is situated in the major groove, oriented perpendicular to the long axis of the DNA. Residues N302 and R304 within the conserved WFXNXR motif of Hα3 form bidentate contacts with adenine and the DNA backbone atoms, respectively (*46*). Another hallmark residue R235 in the N-terminal arm of the homeodomain (*47*, *48*) forms both base-specific and nonspecific DNA−backbone hydrogen bonds within the minor groove (Figure 2B). Even though the exact details of the DNA binding mode vary among different homeodomains (*22*), the signature residue R235 always protrudes deep into the minor groove and makes an extensive and nondiscriminatory hydrogen-bonding network with the base and sugar atoms. R235 has the dual function of DNA binding and serving as part of the NLS, and it adopts a fixed conformation only upon DNA binding, as shown by the comparison of the NMR structure of free HNF1β homeodomain (PDB code 2DA6; unpublished) and our crystal structure in complex with DNA (Figure 2B). In HNF1β, these interactions are further stabilized by the R232 residue, which makes additional hydrogen bonds with DNA backbone atoms (Figures 2B and 3).

POU_S domain sequences among POU transcription factor family members vary far more than homeodomain sequences. As a result, POU_S−DNA interactions are more diverse among the members and provide specificity in DNA target recognition (*12*, *14*). HNF1α and HNF1β are so divergent that they were only recognized as POU transcription factors once the crystal structure of HNF1α became available (*15*). In HNF1β, the signature POU_S−DNA interactions are also observed. For example, highly conserved glutamines Q136 and Q147 (Figures 3 and 5B) create an intricate network of hydrogen bonds with target adenine nucleotide and with each other. Bidentate hydrogen bonds between the Q147 side chain and adenine, a hallmark of POU_S−DNA interactions, are accepted from N6 and donated to N7, and Q136 forms hydrogen bonds with the backbone phosphodiester oxygen of the same base. These interactions are further stabilized by the hydrogen bond between NE2 of Q147 and OE1 of Q136, creating a characteristic three-way interaction (Figure 5B). Additional POU_S−DNA interactions are distinct from those made by Oct-1 and Pit-1, including unique base-specific interactions with S142, N146, and S148 as well as DNA backbone interactions with R137, N155, K156, and K164 (Figure 3).

In comparison with HNF1α−DNA interactions (*15*), HNF1β uses the same residues for base-specific DNA recognition (Figure 3) to the same promoter we used for crystallization. However, backbone recognition is slightly

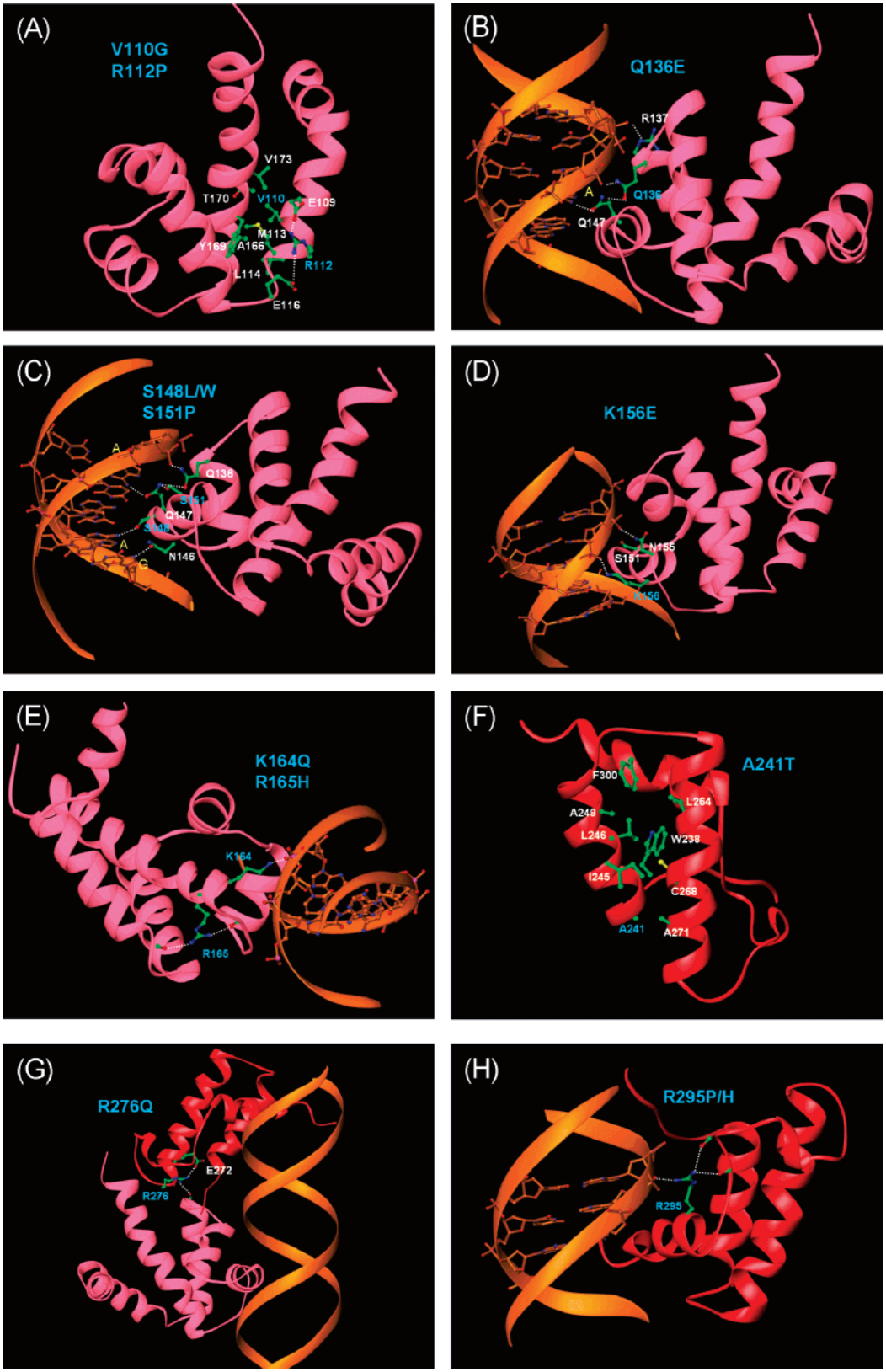

FIGURE 5: Close-up views of each mutation and surrounding residues. The mutated residues are labeled in light blue, while the surrounding residues are labeled in white. DNA bases that make sequence-specific interactions are also labeled in yellow. Ionic interactions and hydrogen bonds are indicated by dotted lines. POU_S is shown in pink, while POU_H is shown in red.

different despite high sequence identity. The same residues display a different mode of DNA backbone interactions. This flexibility and versatility in backbone interactions could account for different target gene selectivity between HNF1α and HNF1*β*. Only a few water molecules have been identified in the HNF1*β*/DNA complex structure due to the modest resolution of the crystals.

Disease-Related Mutations. More than 30 disease-causing mutations have been reported for *HNF1β*; they include missense, nonsense, frameshift, insertion/deletions, and splice

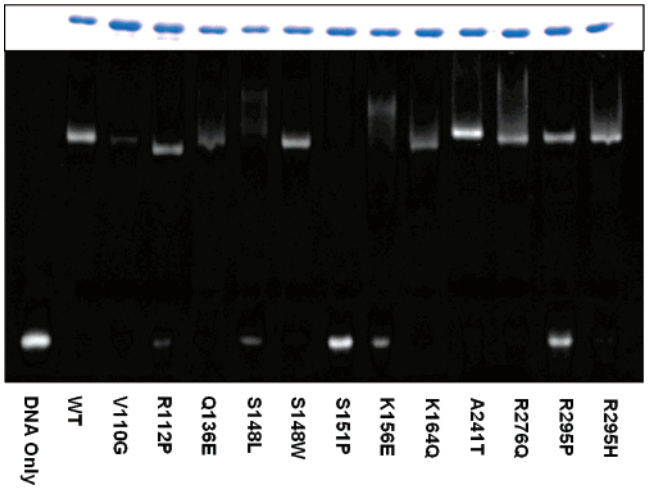

FIGURE 6: DNA binding assay. The amount of loaded protein sample is shown in the top box (Coomassie blue staining). In the main gel, the lower bands correspond to free DNA while the upper bands represent the shifted HNF1β/DNA complex. Wild type (WT) is shown in the second lane as a control, and R165H is missing from the experiment due to an extremely low yield during purification.

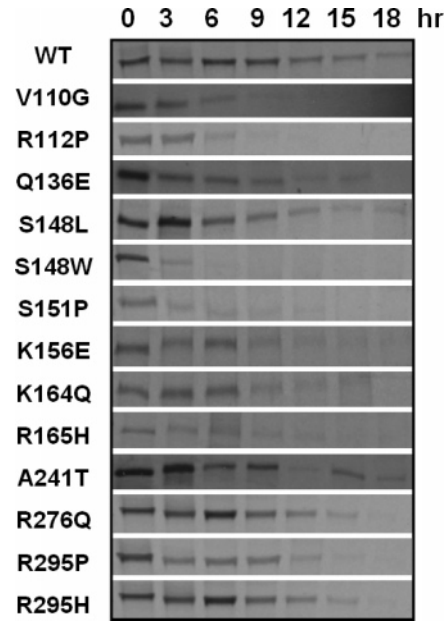

FIGURE 7: Lifetime of the HNF1β mutants compared with wild type. HeLa cells were labeled with [^{35}S]methonine/cysteine for 30 min (0 h) and pulse−chased for various lengths of time (3−18 h) in the presence of excess nonradioactive methionine/cysteine. Samples were immunoprecipitated under normal stringency conditions with polyclonal anti-HNF1β antibody and subjected to SDS−PAGE followed by autoradiography.

site mutations (*24*). Nonsense and frameshift mutations are distributed sporadically throughout the *HNF1β* coding sequence, while missense mutations and the encoded single amino acid substitutions cluster strikingly within the DNA binding domain (Figure 1A). Thirteen out of 16 point (missense) mutations are found within the DNA binding domain, and some of the mutations such as S148L/W, K156E, K164Q, R165H, and R295H/P occur on the corresponding residues in HNF1α, although with different amino acid substitutions (Figure 1B). These point mutations are of great interest because they can be quite instructive as site-specific measures of protein structure and function. They have been mapped onto the HNF1β structure (Figure 4), and the atomic details of individual mutated residues (13 mutations occur on 11 residues) and the surrounding residues are displayed as ball-and-stick models in Figure 5.

The majority (seven out of 11 mutated residues) are located at or near the DNA binding interface, and they are expected to disrupt DNA interactions either directly or indirectly by perturbing local environment (Figure 4). Among these, five residues are directly involved in DNA recognition (Figure 3). S148L/W in the POU_S domain are predicted to disrupt base-specific hydrogen bonds with DNA, whereas cationic side-chain/phosphate backbone interactions are disrupted by Q136E, K156E, and K164Q substitutions in the POU_S domain and R295P/H substitutions in the POU_H domain. All disease-causing mutants exhibited altered DNA binding ability to different degrees except A241T, which appears to retain full DNA binding activity (Figure 6). A241 lies at the fringe of the lining of hydrophobic residues that makes up the core of POU_H (Figure 5F), and a threonine residue can be accommodated at this position. Thus, the A241T mutation has a minimal effect on protein stability (Figure 7) and its effect on transcriptional activity cannot be readily explained (Figure 8). A possibility of interfering with proper recruitment of coactivators cannot be ruled out (*42*, *49*).

Two different mutations found at the adenine-recognizing residue S148 within the POU_S domain (Figure 5C) produce different effects. The S148L mutant loses most of its DNA binding activity, while the S148W mutant retain over 90% DNA binding activity (Figure 6). It is possible that the substituted Trp can still participate in interactions with the adenine base, while the substituted leucine cannot. Trp residues are often found to be involved in base-atom recognition in many protein/DNA complex structures (*50*). However, the S148W mutant has a drastically reduced lifetime compared to wild type (Figure 7), and as a result, it has very low transcriptional activity despite retention of DNA binding (Figure 8). In HNF1α, the corresponding mutant, S142F, was defective in DNA binding despite near-normal protein expression levels (*51*).

R295H and R295P within the POU_H domain also showed a noticeable difference in DNA binding activity in which R295H retained considerable DNA binding activity while R295P lost the majority (Figure 6). This could be due to the loss of the salt bridge with a DNA backbone atom and the distortion of backbone torsion angles by R295P, while R295H retains the salt bridge (but weaker due to lower p*I* of the side chain) (Figure 5H). The lifetime of the R295H mutant was comparable to that of wild type (Figure 7). Furthermore, our data indicated that R295H still retained around 50% overall transcriptional activity relative to wild type (Figure 8). These results might indicate that there is a relatively high threshold for sufficient transcription, or alternatively, the activation level could be gene-specific and the expression of essential genes is below the level needed for proper development and function with the mutant. It has been reported that the R295H mutant exhibited target-specific effects of activation in which the transactivation potential of R295H on the *HNF4α* promoter reached to wild-type transactivation level, while transactivation of either *Afp* or *albumin* promoter by this mutant were barely detectable (*49*). In other studies, the corresponding mutants R263C/L in

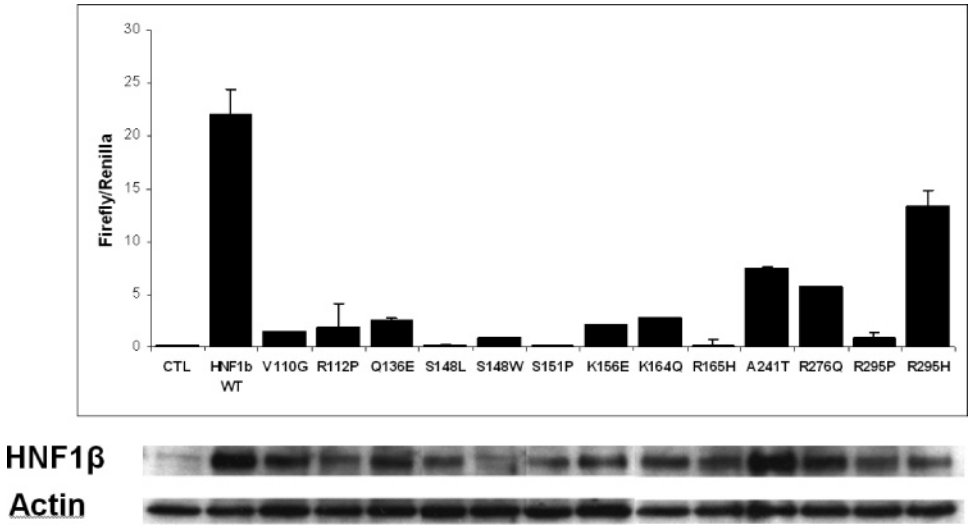

FIGURE 8: Overall transcriptional activity by the mutants compared to wild type. CTL in the first lane refers to an empty vector, and all data have been normalized against firefly/*Renilla* luciferase activity. Protein expression levels were assessed by Western blot and there is a high degree of correlation between these in vivo expression levels and the findings from the protein lifetime assays (Figure 7). Actin, a housekeeping gene product, was used as a loading control.

*HNF1*α showed greatly reduced DNA binding activity as a result of these more drastic substitutions (*52*, *53*).

Another notable DNA binding disrupter is S151P. Even though S151 does not directly contact DNA, it forms a hydrogen bond with the invariant residue Q147 as part of the characteristic three-way interactions with adenine and Q136 within the POU_S domain (Figure 5C). Thus, we expect that the S151P mutation should alter DNA binding by influencing neighboring residues that directly contact DNA. Indeed, no DNA binding was detected (weakest of all, Figure 6), and also a very short protein lifetime was observed (Figure 7). It is believed that the local packing is disturbed by the effect of the proline on backbone torsion angles. As a result, the S151P mutant displayed the lowest overall transcriptional activity in our studies (Figure 8), consistent with the previous findings in which severe clinical phenotypes and complete loss of DNA binding have been reported (*7*, *54*).

The remaining *HNF1β* mutations are predicted to affect either POU_S-POU_H domain interactions or protein stability. Interdomain interaction disruption is expected from the R276Q substitution (Figures 4 and 5G). This mutation interferes with the hydrogen bonds to H130 backbone carbonyl oxygen across the interface as well as the salt bridge to E272. Substitutions at this site noticeably diminished transcriptional activity (Figure 8), despite little effect on protein lifetime (Figure 7). The partial loss of DNA binding activity (Figure 6) should account for the apparent phenotype. It is remarkable that a subtle substitution at this strategic position can have such significant impact on biology.

The *HNF1β* mutations in the final set are predicted to disrupt protein folding or stability, which can lead to accumulation of misfolded protein or premature degradation. Some mutations such as V110G in the POU_S domain, potentially perturb the hydrophobic core, whereas R112P disrupts the ionic interactions and backbone geometry critical to POU_S domain stability. V110 is located in the middle of Pα1 and participates in formation of the hydrophobic core of the POU_S domain, while R112 forms a set of salt bridges with the neighboring residues E109 and E116 (Figure 5A). Replacement by glycine and proline, respectively, is expected to disrupt the hydrophobic core/neighboring ionic interactions as well as the backbone geometry, decreasing protein stability. These mutants showed substantially reduced lifetime (Figure 7) and transcriptional activity (Figure 8). Another mutant that affects protein lifetime is the R165H substitution. R165 is a surface residue bridging two ends of the POU_S domain by forming a pair of hydrogen bonds between the guanidinium group nitrogens and the backbone carbonyl oxygens at either side (Figure 5E). This appears to be critical for integrity and stability of HNF1*β*, as shown by the protein lifetime (Figure 7) and transcription assays (Figure 8). As such, despite repeated trials, we were not able to purify detectable amount of R165H recombinant protein, and the DNA binding could not be assessed. Similar findings were made with the corresponding mutant R159Q in *HNF1*α (*51*, *55*).

A cluster of basic residues at the N-terminus of the homeodomain generally serves as an NLS (*56*). Internal residues in HNF1α and HNF1*β* serve this purpose, as demonstrated by the R200Q/W and R203C/H MODY mutations in *HNF1*α (*55*, *57*). No mutations within this functional region are found in *HNF1β*, however. Thus, *HNF1β* mutations appear to primarily affect DNA target recognition including properly anchoring both domains for optimal DNA recognition and protein stability. The observed effects of all 13 mutations are summarized in Table 2.

In summary, structural studies of the HNF1*β*/DNA complex reported here, together with the earlier-reported structure of the HNF1α/DNA complex (*15*), have revealed the unique features that distinguish these proteins from typical POU transcription factors. In addition, our structures have shed light on how subtle defects in molecular mechanisms can result in severe clinical phenotypes. Although having different effects on DNA binding capacity, all 13 mutants displayed significantly reduced overall transcriptional activity, indicating that these *HNF1β* disease-causing mutations impair organ development/function by a loss-of-function mechanism. These effects on transcriptional activity could be gene-specific or synergistic partner-dependent. It has been

Table 2: HNF1β Point Mutations within the DNA Binding Domain and Their Effects[a]

mutation	phenotype	ref(s)	effects
V110G	glomerulocystic kidney disease	*24*	PS/DB
R112P	diabetes (MODY5	*8, 49*	PS/DB
Q136E	diabetes (MODY5, cortical renal atrophy	*8, 49*	DB/PS
S148L	diabetes (MODY5, renal dysplasia	*24*	DB
S148W	neonatal diabetes, renal cyst	*61*	PS
S151P	renal cysts/genital track malformation	*7, 54*	DB[b]/PS[b]
K156E	diabetes, renal cyst	*24*	DB/PS
K164Q	diabetes (MODY5, enlarged glomeruli	*8, 49*	DB/PS
R165H	diabetes (MODY5, bicornuate uterus	*8, 49*	PS/DB(?)
A241T	diabetic nephropathy	*62*	
R276Q	diabetes, renal cyst	*24, 63*	ID/DB
R295P	diabetes (MODY5, renal cyst	*24*	DB
R295H	diabetes (MODY5, glomerular cyst	*8, 49*	DB

[a] Order of the effects is major to minor from left to right. DB, DNA binding disruptor; PS, protein stability disruptor; ID, interdomain interaction disruptor. [b] Complete loss of DNA binding activity and lowest protein stability.

reported that the effects on transcription of some of these mutants, especially those that do not affect or only weakly affect the DNA-binding activity, correlate with the loss of association with the transcriptional coregulators such as CBP or PCAF (*49*). Thus, even though the molecular bases of the functional disruptions have been elucidated, other mechanistic details that might be exploited for intervention await additional studies. Structural and functional data suggest that the key residues, including the mutational hotspot arginine residues in POU_H (*22*), might be targeted for small molecule or peptide development (*58*, *59*) in order to correct the defects in afflicted individuals or enhance the pancreatic β-cell function.

ACKNOWLEDGMENT

We thank the staff at SER-CAT beamline 22-BM for data collection. We are grateful to David Rodgers for sharing facilities and for critical review of the manuscript. We also thank Dan Noonan for his assistance in the transcriptional reporter assays, and Becky Dutch for her assistance in the pulse−chase experiments.

REFERENCES

1. Yamagata, K. (2003) Regulation of pancreatic beta-cell function by the HNF transcription network: lessons from maturity-onset diabetes of the young (MODY), *Endocr. J. 50*, 491−499.
2. Malecki, M. T. (2005) Genetics of type 2 diabetes mellitus, *Diabetes Res. Clin. Pract. 68* (Suppl. 1), S10−21.
3. Giuffrida, F. M., and Reis, A. F. (2005) Genetic and clinical characteristics of maturity-onset diabetes of the young, *Diabetes Obes. Metab. 7*, 318−326.
4. Chakrabarti, S. K., and Mirmira, R. G. (2003) Transcription factors direct the development and function of pancreatic beta cells, *Trends Endocrinol. Metab. 14*, 78−84.
5. Edghill, E. L., Bingham, C., Slingerland, A. S., Minton, J. A., Noordam, C., Ellard, S., and Hattersley, A. T. (2006) Hepatocyte nuclear factor-1 beta mutations cause neonatal diabetes and intrauterine growth retardation: support for a critical role of HNF-1beta in human pancreatic development, *Diabetic Med 23*, 1301−1306.
6. Horikawa, Y., Iwasaki, N., Hara, M., Furuta, H., Hinokio, Y., Cockburn, B. N., Lindner, T., Yamagata, K., Ogata, M., Tomonaga, O., Kuroki, H., Kasahara, T., Iwamoto, Y., and Bell, G. I. (1997) Mutation in hepatocyte nuclear factor-1 beta gene (TCF2) associated with MODY, *Nat. Genet. 17*, 384−385.
7. Bohn, S., Thomas, H., Turan, G., Ellard, S., Bingham, C., Hattersley, A. T., and Ryffel, G. U. (2003) Distinct molecular and morphogenetic properties of mutations in the human HNF1beta gene that lead to defective kidney development, *J. Am. Soc. Nephrol. 14*, 2033−2041.
8. Bellanne-Chantelot, C., Chauveau, D., Gautier, J. F., Dubois-Laforgue, D., Clauin, S., Beaufils, S., Wilhelm, J. M., Boitard, C., Noel, L. H., Velho, G., and Timsit, J. (2004) Clinical spectrum associated with hepatocyte nuclear factor-1beta mutations, *Ann. Intern. Med. 140*, 510−517.
9. Bingham, C., and Hattersley, A. T. (2004) Renal cysts and diabetes syndrome resulting from mutations in hepatocyte nuclear factor-1{beta}, *Nephrol., Dial., Transplant. 19*, 2703−2708.
10. Igarashi, P., Shao, X., McNally, B. T., and Hiesberger, T. (2005) Roles of HNF-1beta in kidney development and congenital cystic diseases, *Kidney Int. 68*, 1944−1947.
11. Lebrun, G., Vasiliu, V., Bellanne-Chantelot, C., Bensman, A., Ulinski, T., Chretien, Y., and Grunfeld, J. P. (2005) Cystic kidney disease, chromophobe renal cell carcinoma and TCF2 (HNF1 beta) mutations, *Nat. Clin. Pract. Nephrol. 1*, 115−119.
12. Ryan, A. K., and Rosenfeld, M. G. (1997) POU domain family values: flexibility, partnerships, and developmental codes, *Genes Dev. 11*, 1207−1225.
13. Rosenfeld, M. G. (1991) POU-domain transcription factors: pouer-ful developmental regulators, *Genes Dev. 5*, 897−907.
14. Phillips, K., and Luisi, B. (2000) The virtuoso of versatility: POU proteins that flex to fit, *J. Mol. Biol. 302*, 1023−1039.
15. Chi, Y. I., Frantz, J. D., Oh, B. C., Hansen, L., Dhe-Paganon, S., and Shoelson, S. E. (2002) Diabetes mutations delineate an atypical POU domain in HNF-1alpha, *Mol. Cell 10*, 1129−1137.
16. Scully, K. M., Jacobson, E. M., Jepsen, K., Lunyak, V., Viadiu, H., Carriere, C., Rose, D. W., Hooshmand, F., Aggarwal, A. K., and Rosenfeld, M. G. (2000) Allosteric effects of Pit-1 DNA sites on long-term repression in cell type specification, *Science 290*, 1127−1131.
17. Hattersley, A. T., and Pearson, E. R. (2006) Minireview: Pharmacogenetics and Beyond: The Interaction of Therapeutic Response, {beta}-Cell Physiology, and Genetics in Diabetes, *Endocrinology 147*, 2657−2663.
18. Pontoglio, M., Barra, J., Hadchouel, M., Doyen, A., Kress, C., Bach, J. P., Babinet, C., and Yaniv, M. (1996) Hepatocyte nuclear factor 1 inactivation results in hepatic dysfunction, phenylketonuria, and renal Fanconi syndrome, *Cell 84*, 575−585.
19. Pontoglio, M., Sreenan, S., Roe, M., Pugh, W., Ostrega, D., Doyen, A., Pick, A. J., Baldwin, A., Velho, G., Froguel, P., Levisetti, M., Bonner-Weir, S., Bell, G. I., Yaniv, M., and Polonsky, K. S. (1998) Defective insulin secretion in hepatocyte nuclear factor 1alpha-deficient mice, *J. Clin. Invest. 101*, 2215−2222.
20. Shih, D. Q., Screenan, S., Munoz, K. N., Philipson, L., Pontoglio, M., Yaniv, M., Polonsky, K. S., and Stoffel, M. (2001) Loss of HNF-1alpha function in mice leads to abnormal expression of genes involved in pancreatic islet development and metabolism, *Diabetes 50*, 2472−2480.
21. Ryffel, G. U. (2001) Mutations in the human genes encoding the transcription factors of the hepatocyte nuclear factor (HNF)1 and HNF4 families: functional and pathological consequences, *J. Mol. Endocrinol. 27*, 11−29.
22. Chi, Y. I. (2005) Homeodomain revisited: a lesson from disease-causing mutations, *Hum. Genet. 116*, 433−444.
23. Pearson, E. R., Badman, M. K., Lockwood, C. R., Clark, P. M., Ellard, S., Bingham, C., and Hattersley, A. T. (2004) Contrasting diabetes phenotypes associated with hepatocyte nuclear factor-1alpha and -1beta mutations, *Diabetes Care 27*, 1102−1107.
24. Edghill, E. L., Bingham, C., Ellard, S., and Hattersley, A. T. (2006) Mutations in hepatocyte nuclear factor-1{beta} and their related phenotypes, *J. Med. Genet. 43*, 84−90.
25. Kato, N., Toukairin, M., Asanuma, I., and Motoyama, T. (2007) Immunocytochemistry for hepatocyte nuclear factor-1beta (HNF-1beta): A marker for ovarian clear cell carcinoma, *Diagn. Cytopathol. 35*, 193−197.
26. Kato, N., Sasou, S., and Motoyama, T. (2006) Expression of hepatocyte nuclear factor-1beta (HNF-1beta) in clear cell tumors and endometriosis of the ovary, *Mod. Pathol. 19*, 83−89.
27. Beckers, D., Bellanne-Chantelot, C., and Maes, M. (2007) Neonatal cholestatic jaundice as the first symptom of a mutation in the hepatocyte nuclear factor-1beta gene (HNF-1beta), *J. Pediatr. 150*, 313−314.
28. Welters, H. J., Senkel, S., Klein-Hitpass, L., Erdmann, S., Thomas, H., Harries, L. W., Pearson, E. R., Bingham, C., Hattersley, A. T., Ryffel, G. U., and Morgan, N. G. (2006) Conditional expression of hepatocyte nuclear factor-1{beta}, the maturity-onset diabetes of the young-5 gene product, influences the viability and

functional competence of pancreatic {beta}-cells, *J. Endocrinol. 190*, 171−181.
29. Wang, L., Coffinier, C., Thomas, M. K., Gresh, L., Eddu, G., Manor, T., Levitsky, L. L., Yaniv, M., and Rhoads, D. B. (2004) Selective deletion of the Hnf1beta (MODY5) gene in beta-cells leads to altered gene expression and defective insulin release, *Endocrinology 145*, 3941−3949.
30. Senkel, S., Lucas, B., Klein-Hitpass, L., and Ryffel, G. U. (2005) Identification of target genes of the transcription factor HNF1beta and HNF1alpha in a human embryonic kidney cell line, *Biochim. Biophys. Acta 1731*, 179−190.
31. Lu, P., Li, Y., Gorman, A., and Chi, Y. I. (2006) Crystallization of hepatocyte nuclear factor 1beta in complex with DNA, *Acta Crystallogr., Sect. F: Struct. Biol. Cryst. Commun. 62*, 525−529.
32. Vagin, A., and Teplyakov, A. (1997) MOLREP: an automated program for molecular replacement, *J. Appl. Crystallogr. 30*, 1002−1025.
33. Brunger, A. T., Adams, P. D., Clore, G. M., DeLano, W. L., Gros, P., Grosse-Kunstleve, R. W., Jiang, J. S., Kuszewski, J., Nilges, M., Pannu, N. S., Read, R. J., Rice, L. M., Simonson, T., and Warren, G. L. (1998) Crystallography & NMR system: A new software suite for macromolecular structure determination, *Acta Crystallogr. D: Biol. Crystallogr*, *54*, 905−921.
34. Jones, T. A., Zou, J. Y., Cowan, S. W., and Kjeldgaard. (1991) Improved methods for building protein models in electron density maps and the location of errors in these models, *Acta Crystallogr. A 47*, 110−119.
35. Fried, M. G. (1989) Measurement of protein-DNA interaction parameters by electrophoresis mobility shift assay, *Electrophoresis 10*, 366−376.
36. Remenyi, A., Tomilin, A., Scholer, H. R., and Wilmanns, M. (2002) Differential activity by DNA-induced quarternary structures of POU transcription factors, *Biochem. Pharmacol. 64*, 979−984.
37. Remenyi, A., Scholer, H. R., and Wilmanns, M. (2004) Combinatorial control of gene expression, *Nat. Struct. Mol. Biol. 11*, 812−815.
38. Latchman, D. S. (1996) Activation and repression of gene expression by POU family transcription factors, *Philos. Trans. R. Soc. London, B: Biol. Sci. 351*, 511−515.
39. Gunasekaran, K., Tsai, C. J., Kumar, S., Zanuy, D., and Nussinov, R. (2003) Extended disordered proteins: targeting function with less scaffold, *Trends Biochem. Sci. 28*, 81−85.
40. Dunker, A. K., Cortese, M. S., Romero, P., Iakoucheva, L. M., and Uversky, V. N. (2005) Flexible nets. The roles of intrinsic disorder in protein interaction networks, *FEBS J. 272*, 5129−5148.
41. Liu, J., Perumal, N. B., Oldfield, C. J., Su, E. W., Uversky, V. N., and Dunker, A. K. (2006) Intrinsic disorder in transcription factors, *Biochemistry 45*, 6873−6888.
42. Soutoglou, E., Papafotiou, G., Katrakili, N., and Talianidis, I. (2000) Transcriptional activation by hepatocyte nuclear factor-1 requires synergism between multiple coactivator proteins, *J. Biol. Chem. 275*, 12515−12520.
43. Dohda, T., Kaneoka, H., Inayoshi, Y., Kamihira, M., Miyake, K., and Iijima, S. (2004) Transcriptional coactivators CBP and p300 cooperatively enhance HNF-1alpha-mediated expression of the albumin gene in hepatocytes, *J. Biochem. (Tokyo) 136*, 313−319.
44. Mendel, D. B., and Crabtree, G. R. (1991) HNF-1, a member of a novel class of dimerizing homeodomain proteins, *J. Biol. Chem. 266*, 677−680.
45. Tronche, F., Ringeisen, F., Blumenfeld, M., Yaniv, M., and Pontoglio, M. (1997) Analysis of the distribution of binding sites for a tissue-specific transcription factor in the vertebrate genome, *J. Mol. Biol. 266*, 231−245.
46. Wolberger, C. (1996) Homeodomain interactions, *Curr. Opin. Struct. Biol. 6*, 62−68.
47. Gehring, W. J., Qian, Y. Q., Billeter, M., Furukubo-Tokunaga, K., Schier, A. F., Resendez-Perez, D., Affolter, M., Otting, G., and Wuthrich, K. (1994) Homeodomain-DNA recognition, *Cell 78*, 211−223.
48. Shang, Z., Isaac, V. E., Li, H., Patel, L., Catron, K. M., Curran, T., Montelione, G. T., and Abate, C. (1994) Design of a "minimAl" homeodomain: the N-terminal arm modulates DNA binding affinity and stabilizes homeodomain structure, *Proc. Natl. Acad. Sci. U.S.A. 91*, 8373−8377.
49. Barbacci, E., Chalkiadaki, A., Masdeu, C., Haumaitre, C., Lokmane, L., Loirat, C., Cloarec, S., Talianidis, I., Bellanne-Chantelot, C., and Cereghini, S. (2004) HNF1beta/TCF2 mutations impair transactivation potential through altered co-regulator recruitment, *Hum. Mol. Genet. 13*, 3139−3149.
50. Baker, C. M., and Grant, G. H. (2007) Role of aromatic amino acids in protein-nucleic acid recognition, *Biopolymers 85*, 456−470.
51. Vaxillaire, M., Abderrahmani, A., Boutin, P., Bailleul, B., Froguel, P., Yaniv, M., and Pontoglio, M. (1999) Anatomy of a homeoprotein revealed by the analysis of human MODY3 mutations, *J. Biol. Chem. 274*, 35639−35646.
52. Yang, Q., Yamagata, K., Yamamoto, K., Miyagawa, J., Takeda, J., Iwasaki, N., Iwahashi, H., Yoshiuchi, I., Namba, M., Miyazaki, J., Hanafusa, T., and Matsuzawa, Y. (1999) Structure/function studies of hepatocyte nuclear factor-1alpha, a diabetes-associated transcription factor, *Biochem. Biophys. Res. Commun. 266*, 196−202.
53. Kim, K. A., Kang, K., Chi, Y. I., Chang, I., Lee, M. K., Kim, K. W., Shoelson, S. E., and Lee, M. S. (2003) Identification and functional characterization of a novel mutation of hepatocyte nuclear factor-1alpha gene in a Korean family with MODY3, *Diabetologia 46*, 721−727.
54. Bingham, C., Ellard, S., Cole, T. R., Jones, K. E., Allen, L. I., Goodship, J. A., Goodship, T. H., Bakalinova-Pugh, D., Russell, G. I., Woolf, A. S., Nicholls, A. J., and Hattersley, A. T. (2002) Solitary functioning kidney and diverse genital tract malformations associated with hepatocyte nuclear factor-1beta mutations, *Kidney Int. 61*, 1243−1251.
55. Yamada, S., Tomura, H., Nishigori, H., Sho, K., Mabe, H., Iwatani, N., Takumi, T., Kito, Y., Moriya, N., Muroya, K., Ogata, T., Onigata, K., Morikawa, A., Inoue, I., and Takeda, J. (1999) Identification of mutations in the hepatocyte nuclear factor-1alpha gene in Japanese subjects with early-onset NIDDM and functional analysis of the mutant proteins, *Diabetes 48*, 645−648.
56. Boulikas, T. (1994) Putative nuclear localization signals (NLS) in protein transcription factors, *J. Cell. Biochem. 55*, 32−58.
57. Chevre, J. C., Hani, E. H., Boutin, P., Vaxillaire, M., Blanche, H., Vionnet, N., Pardini, V. C., Timsit, J., Larger, E., Charpentier, G., Beckers, D., Maes, M., Bellanne-Chantelot, C., Velho, G., and Froguel, P. (1998) Mutation screening in 18 Caucasian families suggest the existence of other MODY genes, *Diabetologia 41*, 1017−1023.
58. Gniazdowski, M., Denny, W. A., Nelson, S. M., and Czyz, M. (2003) Transcription factors as targets for DNA-interacting drugs, *Curr. Med. Chem. 10*, 909−924.
59. Boger, D. L. (2003) Solution-phase synthesis of combinatorial libraries designed to modulate protein-protein or protein-DNA interactions, *Bioorg. Med. Chem. 11*, 1607−1613.
60. Xu, H. E., Lambert, M. H., Montana, V. G., Parks, D. J., Blanchard, S. G., Brown, P. J., Sternbach, D. D., Lehmann, J. M., Wisely, G. B., Willson, T. M., Kliewer, S. A., and Milburn, M. V. (1999) Molecular recognition of fatty acids by peroxisome proliferator-activated receptors, *Mol. Cell 3*, 397−403.
61. Yorifuji, T., Kurokawa, K., Mamada, M., Imai, T., Kawai, M., Nishi, Y., Shishido, S., Hasegawa, Y., and Nakahata, T. (2004) Neonatal diabetes mellitus and neonatal polycystic, dysplastic kidneys: Phenotypically discordant recurrence of a mutation in the hepatocyte nuclear factor-1beta gene due to germline mosaicism, *J. Clin. Endocrinol. Metab. 89*, 2905−2908.
62. Weng, J. P., Lehto, M., Forsblom, C., Huang, X., Li, H., and Groop, L. C. (2000) Hepatocyte nuclear factor-1 beta (MODY5) gene mutations in Scandinavian families with early-onset diabetes or kidney disease or both, *Diabetologia 43*, 131−132.
63. Furuta, H., Furuta, M., Sanke, T., Ekawa, K., Hanabusa, T., Nishi, M., Sasaki, H., and Nanjo, K. (2002) Nonsense and missense mutations in the human hepatocyte nuclear factor-1 beta gene (TCF2) and their relation to type 2 diabetes in Japanese, *J. Clin. Endocrinol. Metab. 87*, 3859−3863.

BI7010527